RESEARCH ARTICLE

Check for updates

Ionic Conduction in Cold-Sintered Metakaolin Ceramics

Linhao Li[1,2,*], Yinyin Zhang[2], Zibo Xu[2] and Bofeng Li[2]

[1] College of Mathematics and Physics, Beijing University of Chemical Technology, Beijing 100029, China
[2] Beijing Royal School, Beijing 102209, China

Abstract

The influence of process conditions and post-annealing treatments on the ionic transport properties of metakaolin (MK) ceramics prepared by the cold sintering process (CSP) were investigated. Within the temperature range of 120–200 °C, CSP temperature has little influence on densification and microstructure. Impedance spectroscopy revealed that all as-sintered ceramics exhibited significant ionic conduction, with bulk conductivity of approximately 0.001 S/cm at 600 °C. The associated activation energies are confined to a narrow range of 0.63–0.65 eV. In contrast, post-annealing significantly alters the electrical microstructure, giving rise to an additional grain boundary response. After annealing at 1100 °C, the bulk ionic conductivity increased. This increase is likely attributed to the space charge effect due to the coexistence of crystalline and amorphous regions.

Keywords: cold sintering process, metakaolin, ionic conductivity, impedance spectroscopy, space charge effect.

Submitted: 13 April 2026
Accepted: 06 May 2026
Published: 10 May 2026

Vol. 2, **No.** 2, 2026.
10.62762/JAEM.2026.769607

***Corresponding author:**
✉ Linhao Li
linhao.li@mail.buct.edu.cn

1 Introduction

Modern society exhibits an energy-intensive character, with its structure largely being a product of energy conversion, storage and utilisation. The rapid growth of sectors such as electric transportation, artificial intelligence and metallurgy has led to a significant increase in demand for high performance electrochemical equipment. Electrolytes are central to devices such as lithium-ion batteries, fuel cells, supercapacitors, and various electrochemical sensors [1, 2]. Compared to liquid electrolytes, solid electrolytes offer significant improvements in both safety and energy density. Consequently, developing novel solid electrolytes with high ionic conductivity has become a main aim in materials science.

In addition to material properties, sustainability is another key factor influencing materials research. Exploring environmentally friendly and naturally abundant materials is one of the dominant strategies. Metakaolin is an aluminosilicate material obtained through the dehydration of kaolinite, a naturally abundant clay mineral widely distributed in the Earth's crust [3]. Its amorphous structure provides potential pathways for ion migration, enabling it to exhibit ionic conductivity when mobile cations are introduced [4, 5].

The cold sintering process (CSP) is an emerging densification technique that utilises the "dissolution-precipitation" mechanism [6–13]. Under

Citation
Li, L., Zhang, Y., Xu, Z., & Li, B. (2026). Ionic Conduction in Cold-Sintered Metakaolin Ceramics. *Journal of Advanced Electronic Materials*, 2(2), 44–50.

the combined influence of transient liquid phase (TLP) and pressure, it enables materials to be densified at significantly reduced temperatures (typically below 300°C). Compared to conventional high temperature sintering, CSP not only reduces energy consumption, its low temperature characteristics also make it an ideal solution for handling materials susceptible to degradation at high temperatures. Since the cold sintering process (CSP) was first introduced in 2016, it has attracted considerable attention due to its ability to densify ceramics at significantly lower temperatures compared to conventional sintering. The technique has been successfully applied to a wide range of material systems, including microwave dielectric ceramics, ferroelectric and piezoelectric materials, solid-state ionic conductors, and battery components [14–22].

In previous work, MK was successfully densified via CSP, achieving >90% density while preserving its amorphous structure [23]. Notably, considerable bulk ionic conductivity was observed in CSPed ceramic (on the order of 10^{-3} S/cm at 600 °C) [23], indicating that CSPed metakaolin could be a promising candidate for use as a solid-state electrolyte. Compared to synthetic electrolytes, CSPed metakaolin offers significant advantages. Its precursor, kaolinite, is a naturally abundant mineral, ensuring low cost and large-scale availability. Metakaolin itself can be produced via a low-temperature (650 °C) heating, making it both energy-efficient and easy to process, thereby aligning with the goal of sustainable development.

Based on this, the present study aims to investigate the effects of CSP temperature and post-annealing on the ionic conductivity of CSPed MK ceramics. By analysing the relationship between processing conditions and electrical properties and microstructure, this study will provide guidance on optimising processing parameters to improve ionic conductivity.

2 Experimental

The raw powder used in this research was washed metakaolin (MK) powder, sourced from Henan Borun New Materials Co., Ltd. Detailed characterization of the MK powder, including its chemical constituents and physical properties, has been documented in our previous work [23]. The powder was subjected to an overnight drying process at 200 °C before use. To prepare the CSP ceramics, the MK powder was mixed with 5 mol/L NaOH solutions in a weight ratio of 60% using a mortar and pestle for 5 minutes. The resulting mixtures were then transferred into a 10 mm diameter stainless-steel die. The CSP procedure involved an initial compaction at 500 MPa under ambient conditions for 5 minutes. The same pressure was maintained as the die was then heated to 120 - 200 °C at a rate of 10 °C/min. After a 30 min isothermal dwell, the system was cooled naturally to room temperature before the sintered ceramic pellet was removed from the die. The density of MK ceramics was measured by geometric method and corrected for the residual TLP remaining in the sintered MK ceramics based on our previous study.

The samples prepared at different CSP temperatures were denoted as CS120, CS160, and CS200, corresponding to CSP temperatures of 120, 160, and 200 °C, respectively. Selected CS200 samples were further annealed at different temperatures, and these samples were labelled as CS200-A800, CS200-A950, and CS200-A1100, corresponding to annealing temperatures of 800, 950, and 1100 °C, respectively.

Microstructural and elemental evaluations were conducted using a RISE-MAGNA scanning electron microscope (SEM). Complex impedance was measured via an TH2829C LCR meter on pellets coated with 80 °C cured Ag paste and 800 °C cured Au paste. Data were normalized for sample geometry, and high-frequency inductance was mitigated through short-circuit calibration.

3 Results and Discussion

The influence of sintering temperature on the densification of CSP MK ceramics is shown in Figure 1. Within the temperature range of 120–200 °C, the temperature shows very limited influence on the density of the obtained MK ceramics with no clear trend observed. Taking uncertainty into consideration, the differences among these three temperatures are not statistically significant.

SEM observations of both the polished surfaces and fractured surfaces of all three samples indicate relatively good densification, Figure 2. However, a certain number of residual pores can still be observed, consistent with the measured relative densities of ∼85%. Contrast variations are evident in the secondary electron (SE) images of the polished surfaces but not in the corresponding backscattered electron (BSE) images. This suggests that the variations are not related to compositional differences, but rather to surface-related effects such as roughness or charging.

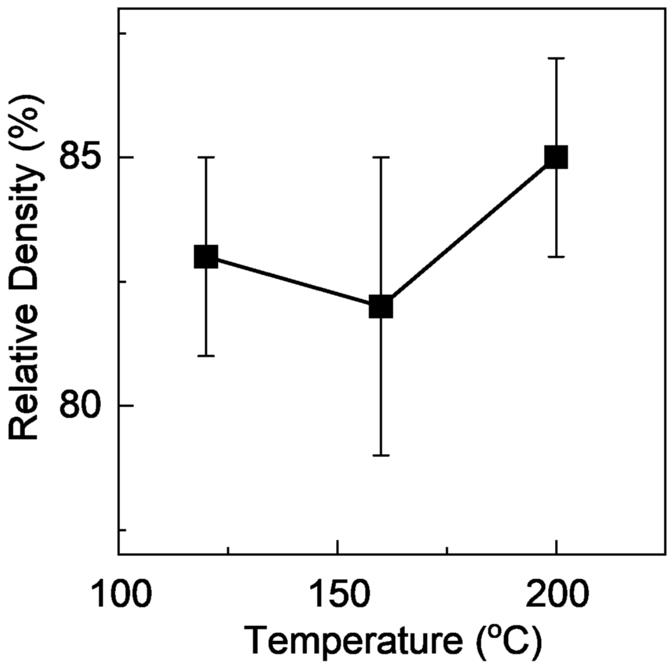

Figure 1. Variation of relative density as a function of CSP temperature.

No clear grain structure is visible in fracture surface images, but some grain features can be distinguished in the BSE images, with sizes roughly in the range of 1–5 μm. Considering that the raw MK powder used in this study has an initial particle size of approximately 1 μm, it can be concluded that only limited grain growth occurs during CSP [23].

Figure 3(a) shows the impedance plot of the as-sintered CSP ceramics. In terms of their electrical microstructure, all three samples consist of two distinguishable components, corresponding to the bulk response (the semicircle) and the electrode effect response (low frequency spike). The presence of the electrode effect confirms that these ceramics possess a significant level of ionic conduction. The bulk conductivity ($\sigma_{\text{bulk}} = 1/\rho_{\text{bulk}}$), obtained from low frequency intercept of impedance plot, is summarized in the Arrhenius plot shown in Figure 4(a). Consistent with previous report, all as-sintered ceramics exhibit a low-temperature plateau. This behaviour is closely related to the presence of residual TLP, as the plateau disappears during the cooling cycle. This plateau arises from competing effects: increasing temperature enhances ion mobility, while simultaneous TLP loss reduces conductive pathways. This leads to a near-constant conductivity in this temperature range. Above 300°C, the conductivity exhibits a linear relationship with the reciprocal of the temperature, demonstrating its thermally excited nature. The highest conductivity was observed in CS200, although all samples reached approximately 0.001 S/cm at 600 °C, with only a modest variation. The activation energies (E_a) extracted from the linear part are confined to a narrow range of 0.63–0.65 eV, which are typical values for ionic conductors. Furthermore, as shown in Figure 3(d), the frequency-dependent M'' spectra of the as-sintered ceramics display bulk relaxation peaks at nearly the same frequencies for all samples, suggesting a similar bulk time constant, which further confirms the similarity of the bulk phases in these ceramics.

Table 1. Shrinkage of CSPed metakaolin (MK) ceramics after annealing at different temperatures.

Annealing Temperature (° C)	Diameter Shrinkage (%)
800	0.2
950	1.1
1100	6.5

To further investigate the electrical conduction mechanism of CSPed MK ceramics, post-annealing was carried out. Although all MK ceramics had already reached a relatively high density after CSP, a certain degree of shrinkage was still observed after annealing. It is known that the amorphous phase in MK begins to crystallise at around 900 °C, forming a mixed phase of mullite, spinel and cristobalite. Due to this phase transformation, densities before and after annealing cannot be compared on a consistent basis. Therefore, Table 1 summarises the shrinkage induced at different annealing temperatures as a reference. The diameter shrinkage increases gradually from 0.2% at 800 °C to 6.5% at 1100 °C. This suggests that significant densification only occurs at 1100 °C, with negligible shrinkage at lower temperatures.

On the other hand, post-annealing has a significant impact on the electrical microstructure of CSP ceramics. Figure 3(b, c) shows the evolution of the impedance plot of the CS200 sample after annealing. The most significant change is the appearance of an additional electroactive region (semicircle) in the impedance plot. Based on the corresponding capacitance values ($\sim 1 \times 10^{-10}\,\mathrm{F\,cm^{-1}}$), this new component can be reasonably attributed to the grain boundary response. With increasing annealing temperature, the grain boundary resistance gradually increases, indicating a progressive evolution of the electrical microstructure.

In contrast, only negligible shrinkage is observed below

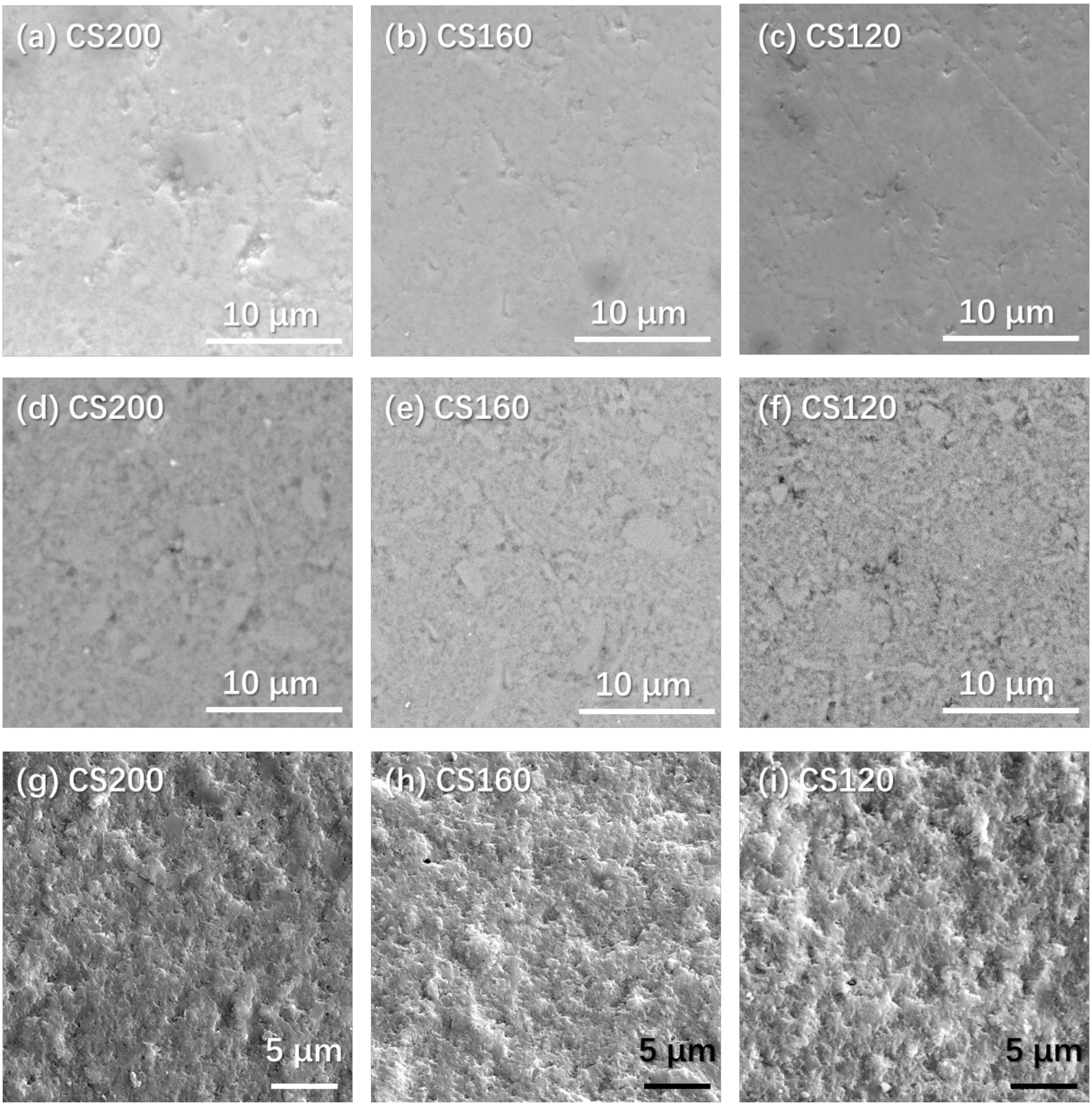

Figure 2. (a–c) Secondary electron images and (d–f) backscattered electron images of polished surfaces of CSP ceramics sintered at 200, 160 and 120 °C, respectively; (g–i) fractured surfaces of CSP ceramics sintered at 200, 160 and 120 °C, respectively.

1100 °C (see Table 1), suggesting that these changes are not significantly associated with densification. This behaviour may be related to the presence of certain conductive residual species located at the grain boundaries in the as-sintered ceramics (e.g., residual NaOH solution from TLP), which were introduced during the CSP process and initially enhance grain boundary conduction. Upon annealing, these residual species are removed through volatilization or undergo chemical reaction to form a less conductive phase(s), thereby reducing their contribution to grain boundary transport.

As can be seen from the σ_{bulk} in Figure 4(b) and the time constants in Figure 3(e), the bulk response is relatively unaffected by the annealing process. The persistence of low frequency spike associated with the electrode effect further confirms that ionic conduction continues to dominate in these ceramics. The σ_{bulk} of CS200, CS200-A800 and CS200-A950

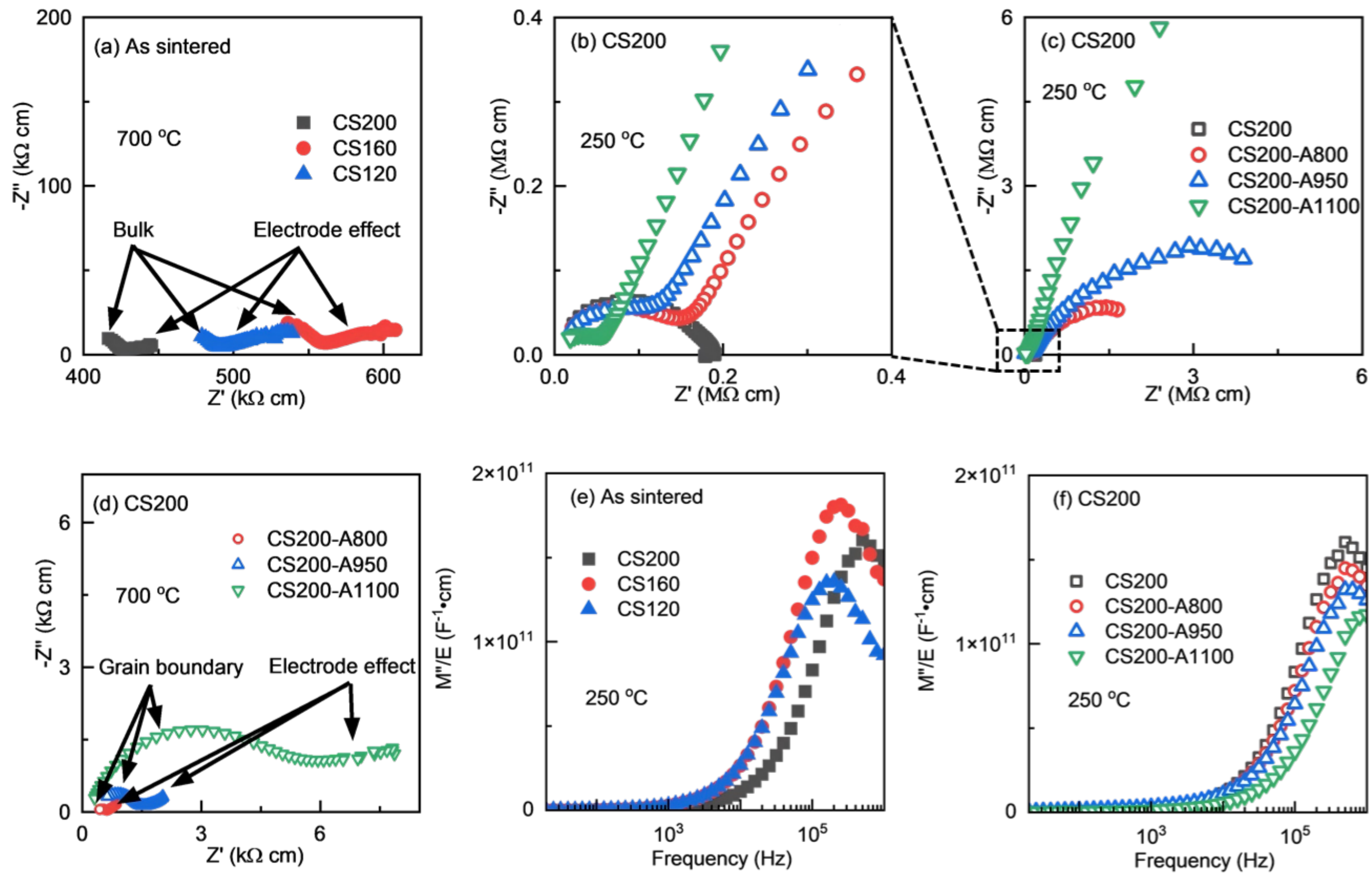

Figure 3. Impedance plots of (a) as-sintered ceramics and (b, c, e) post-annealed ceramics. Frequency-dependent M'' modulus plots of (d) as-sintered ceramics and (f) post-annealed ceramics.

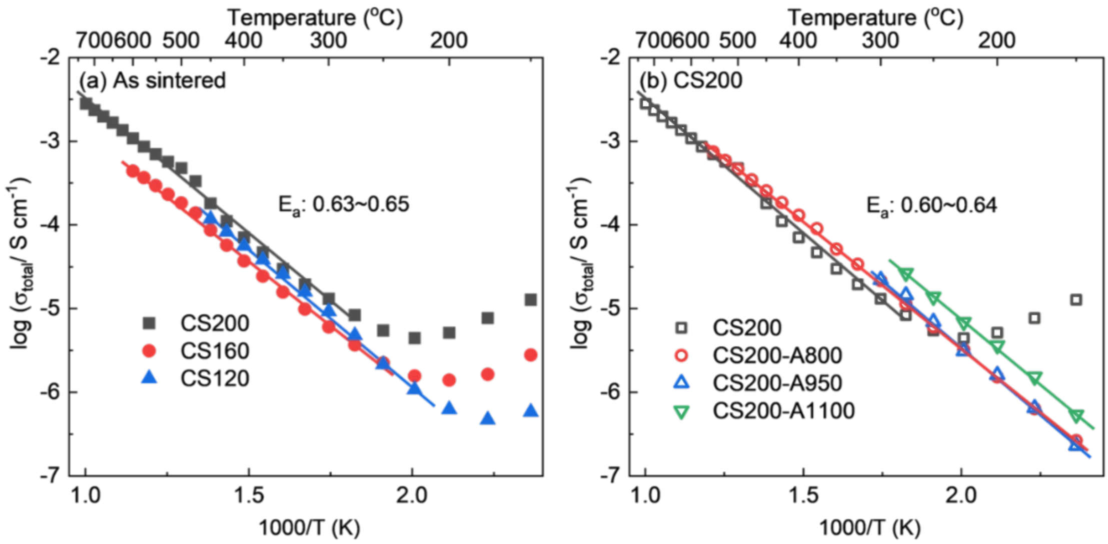

Figure 4. Arrhenius plots of bulk conductivity for (a) as-sintered ceramics and (b) post-annealed ceramics.

are comparable to each other, with the highest value observed in CS200-A1100. This outcome is somewhat unexpected, given that MK typically begins to crystallise at temperatures above 900 °C, forming spinel and mullite phases. Since these phases are generally regarded as electrically insulating and unable to support significant ionic transport, it is therefore expected that a certain level of residual amorphous SiO_2 will remain in the CS200-A1100 sample. In this case, the observed increase in σ_{bulk} of CS200-A1100 is likely also associated with the formation of fine crystallite phases. The interfaces formed between the new crystallised phases and the remaining amorphous SiO_2 can induce space charge effect [24], which have been demonstrated to facilitate fast ionic migration at the interface [25–27] and thereby enhance the effective ionic conductivity of the ceramic.

4 Conclusion

This study demonstrates that the CSP temperature within the range of 120–200 °C has only a minor impact on the densification, microstructure, and bulk conduction property. All as-sintered samples exhibit similar electrical behaviour, with E_a of 0.63–0.65 eV, which indicates consistent ionic transport mechanisms. In contrast, post-annealing significantly alters the electrical microstructure. The appearance of a grain boundary response after annealing indicates the progressive removal or transformation of residual TLP. Higher annealing temperature leads to higher grain boundary resistance, while the bulk conductivity remains largely unchanged.

Data Availability Statement

Data will be made available on request.

Funding

This work was supported without any funding.

Conflicts of Interest

The authors declare no conflicts of interest.

AI Use Statement

The authors declare that no generative AI was used in the preparation of this manuscript.

Ethical Approval and Consent to Participate

Not applicable.

References

[1] Janek, J., & Zeier, W. G. (2016). A solid future for battery development. *Nature energy, 1*(9), 1-4. [CrossRef]

[2] Bachman, J. C., Muy, S., Grimaud, A., Chang, H. H., Pour, N., Lux, S. F., ... & Shao-Horn, Y. (2016). Inorganic solid-state electrolytes for lithium batteries: mechanisms and properties governing ion conduction. *Chemical reviews, 116*(1), 140-162. [CrossRef]

[3] Jiang, T., Liu, Z., Tian, X., Wu, J., & Wang, L. (2024). Review on the impact of metakaolin-based geopolymer's reaction chemistry, nanostructure and factors on its properties. *Construction and Building Materials, 412*, 134760. [CrossRef]

[4] Souquet, J. L. (1981). Ionic transport in amorphous solid electrolytes. *Annual Review of Materials Science, 11*(1), 211-231. [CrossRef]

[5] Nascimento, M. L. F., Rodrigues, A. C. M., & Souquet, J. L. (2010). Microscopic and thermodynamic interpretations of experimental data on ionic conductivity in lithium silicate glasses. *Physics and Chemistry of Glasses-European Journal of Glass Science and Technology Part B, 51*(1), 69-77.

[6] Guo, J., Berbano, S. S., Guo, H., Baker, A. L., Lanagan, M. T., & Randall, C. A. (2016). Cold sintering process of composites: bridging the processing temperature gap of ceramic and polymer materials. *Advanced Functional Materials, 26*(39), 7115-7121. [CrossRef]

[7] Guo, J., Floyd, R., Lowum, S., Maria, J. P., Herisson de Beauvoir, T., Seo, J. H., & Randall, C. A. (2019). Cold sintering: progress, challenges, and future opportunities. *Annual Review of Materials Research, 49*(1), 275-295. [CrossRef]

[8] Guo, J., Baker, A. L., Guo, H., Lanagan, M., & Randall, C. A. (2017). Cold sintering process: a new era for ceramic packaging and microwave device development. *Journal of the American Ceramic Society, 100*(2), 669-677. [CrossRef]

[9] Maria, J. P., Kang, X., Floyd, R. D., Dickey, E. C., Guo, H., Guo, J., ... & Randall, C. A. (2017). Cold sintering: Current status and prospects. *Journal of Materials Research, 32*(17), 3205-3218. [CrossRef]

[10] Guo, H., Guo, J., Baker, A., & Randall, C. A. (2016). Hydrothermal-assisted cold sintering process: a new guidance for low-temperature ceramic sintering. *ACS applied materials & interfaces, 8*(32), 20909-20915. [CrossRef]

[11] Guo, H., Baker, A., Guo, J., & Randall, C. A. (2016). Cold sintering process: a novel technique for low-temperature ceramic processing of ferroelectrics. *Journal of the American Ceramic Society, 99*(11), 3489-3507. [CrossRef]

[12] Zubairi, H., Hussain, F., Sheikh, S., Shaikh, A. A., Wang, D., & Reaney, I. M. (2023). Comparative study of cold assisted and conventional sintering of (1-2x) K0. 5Na0. 5NbO3-xBaTiO3-xBiFeO3 multiferroic ceramics. *Materials Science and Engineering: B, 296*, 116632. [CrossRef]

[13] Ndayishimiye, A., Sengul, M. Y., Sada, T., Dursun, S., Bang, S. H., Grady, Z. A., ... & Randall, C. A. (2020). Roadmap for densification in cold sintering: Chemical pathways. *Open Ceramics, 2*, 100019. [CrossRef]

[14] Funahashi, S., Guo, J., Guo, H., Wang, K., Baker, A. L., Shiratsuyu, K., & Randall, C. A. (2017). Demonstration of the cold sintering process study for the densification and grain growth of ZnO ceramics. *Journal of the American Ceramic Society, 100*(2), 546-553. [CrossRef]

[15] Tsuji, K., Ndayishimiye, A., Lowum, S., Floyd, R., Wang, K., Wetherington, M., ... & Randall, C. A. (2020). Single step densification of high permittivity BaTiO3

ceramics at 300 ºC. *Journal of the European Ceramic Society, 40*(4), 1280-1284. [CrossRef]

[16] Wang, D., Li, L., Jiang, J., Lu, Z., Wang, G., Song, K., ... & Reaney, I. M. (2021). Cold sintering of microwave dielectric ceramics and devices. *Journal of Materials Research, 36*(2), 333-349. [CrossRef]

[17] Zaengle, T. H., Ndayishimiye, A., Tsuji, K., Fan, Z., Bang, S. H., Perini, J., ... & Randall, C. A. (2020). Single-step densification of nanocrystalline CeO2 by the cold sintering process. *Journal of the American Ceramic Society, 103*(5), 2979-2985. [CrossRef]

[18] Zhao, X., Guo, J., Wang, K., Herisson De Beauvoir, T., Li, B., & Randall, C. A. (2018). Introducing a ZnO–PTFE (polymer) nanocomposite varistor via the cold sintering process. *Advanced Engineering Materials, 20*(7), 1700902. [CrossRef]

[19] Seo, J. H., Guo, J., Guo, H., Verlinde, K., Heidary, D. S. B., Rajagopalan, R., & Randall, C. A. (2017). Cold sintering of a Li-ion cathode: LiFePO4-composite with high volumetric capacity. *Ceramics International, 43*(17), 15370-15374. [CrossRef]

[20] Li, L., Andrews, J., Mitchell, R., Button, D., Sinclair, D. C., & Reaney, I. M. (2023). Aqueous cold sintering of Li-based compounds. *ACS Applied Materials & Interfaces, 15*(16), 20228-20239. [CrossRef]

[21] Liu, B., Li, L., Song, K. X., Mao, M. M., Lu, Z., Wang, G., ... & Reaney, I. M. (2021). Enhancement of densification and microwave dielectric properties in LiF ceramics via a cold sintering and post-annealing process. *Journal of the European Ceramic Society, 41*(2), 1726-1729. [CrossRef]

[22] Seo, J. H., Verlinde, K., Rajagopalan, R., Gomez, E. D., Mallouk, T. E., & Randall, C. A. (2019). Cold sintering process for fabrication of a high volumetric capacity Li4Ti5O12 anode. *Materials Science and Engineering: B, 250*, 114435. [CrossRef]

[23] Li, L., Yang, F., Liu, C., Chen, Z., Ge, J., & Hou, Z. (2025). Cold Sintering of Metakaolin: a One-Step Densification Process of Amorphous Aluminosilicate. *Ceramics International, 51*(24), 43311–43318. [CrossRef]

[24] Liang, C. C. (1973). Conduction characteristics of the lithium iodide-aluminum oxide solid electrolytes. *Journal of the Electrochemical Society, 120*(10), 1289-1292. [CrossRef]

[25] Maier, J. (1995). Ionic conduction in space charge regions. *Progress in solid state chemistry, 23*(3), 171-263. [CrossRef]

[26] Maier, J. (1984). Surface Induced Defects in the Space Charge Region and the Enhancement of Ionic Conductivity in Two-Phase Systems. *physica status solidi (b), 123*(1), K89-K91. [CrossRef]

[27] Maier, J. (1985). Space charge regions in solid two-phase systems and their conduction contribution—I. Conductance enhancement in the system ionic conductor-'inert'phase and application on AgC1: Al2O3 and AgC1: SiO2. *Journal of Physics and Chemistry of Solids, 46*(3), 309-320. [CrossRef]

Linhao Li is a faculty member at the College of Mathematics and Physics, Beijing University of Chemical Technology. He received his PhD in Materials Science and Engineering from the University of Sheffield. His research interests focus on the electrical microstructure and defect chemistry of electronic ceramics through advanced electrical characterization techniques, particularly impedance spectroscopy. He is dedicated to the design of novel materials by exploring the relationships between composition, structure, and performance. (Email: linhao.li@mail.buct.edu.cn)

Yinyin Zhang is a student at Beijing Royal School, China. She is interested in materials science, particularly polymer synthesis and applications, the preparation of composite materials, and basic studies of functional materials. In her extracurricular studies, she has dedicated herself to the fundamental principles and preparation methods in these fields, and her findings are expected to find applications in advanced materials and environmental science. (Email: zhangyinyin@st.brs.edu.cn)

Zibo Xu is a student at Beijing Royal School, China. He is interested in soil-based functional materials, electrolytic conductors, and their applications. In his research under the supervision of Dr. Linhao Li, he explores the conductive properties of Kaolin-based electrolytic systems and their potential use in advanced electrochemical devices. (Email: xuzibo@st.brs.edu.cn)

Bofeng Li is a student at Beijing Royal School, China. He is interested in inorganic chemistry, organic chemistry, materials science, and environmental science. In his extracurricular studies, he explores the synthesis and applications of novel materials, the development of environmentally friendly materials, and their potential applications in energy and environmental protection. (Email: libofeng@st.brs.edu.cn)